arXiv:1111.7096v1 [cond-mat.mes-hall] 30 Nov 2011

Multifractal analysis of the electronic states in the Fibonacci superlattice under weak electric fields

M. Wołoszyn,[*] B.J. Spisak

AGH University of Science and Technology,
Faculty of Physics and Applied Computer Science,
al. A. Mickiewicza 30, 30-059 Krakow, Poland

Abstract

Influence of the weak electric field on the electronic structure of the Fibonacci superlattice is considered. The electric field produces a nonlinear dynamics of the energy spectrum of the aperiodic superlattice. Mechanism of the nonlinearity is explained in terms of energy levels anticrossings. The multifractal formalism is applied to investigate the effect of weak electric field on the statistical properties of electronic eigenfunctions. It is shown that the applied electric field does not remove the multifractal character of the electronic eigenfunctions, and that the singularity spectrum remains non-parabolic, however with a modified shape. Changes of the distances between energy levels of neighbouring eigenstates lead to the changes of the inverse participation ratio of the corresponding eigenfunctions in the weak electric field. It is demonstrated, that the local minima of the inverse participation ratio in the vicinity of the anticrossings correspond to discontinuity of the first derivative of the difference between marginal values of the singularity strength. Analysis of the generalized dimension as a function of the electric field shows that the electric field correlates spatial fluctuations of the neighbouring electronic eigenfunction amplitudes in the vicinity of anticrossings, and the nonlinear character of the scaling exponent confirms multifractality of the corresponding electronic eigenfunctions.

1 Introduction

Statistical properties of the electronic states in nanosystems are a subject of great interest (see, for example, Refs. [1, 2, 3, 4] and the references therein). Partially it is due to the progress of experimental methods of nanophysics which allows to intentionally fabricate high-quality heterostructures consisting of alternating layers of different materials [5, 6, 7, 8]. The thickness of each layer can be controlled during the growth process with accuracy of one atomic monolayer, so that one can fabricate multilayer systems (superlattices) with the desired geometrical parameters of layers and well defined interfaces. In this way periodic as well as disordered multilayer systems can be obtained by the sequential deposition of layers with different thickness of material.

An intermediate case between periodic and disordered multilayer systems corresponds to aperiodic order of layers [9, 10]. Such structures are intentionally generated by the deposition of layers of two different materials according to the Fibonacci, Rudin-Shapiro, Thue-Morse, etc. sequences [11, 12, 13, 14, 15, 16, 17, 18, 19, 20, 21, 22, 23]. Experimental as well as theoretical studies of these superlattices are concentrated on the consequences of the long-range correlations induced by the aperiodic arrangement at a length scale longer than atomic one [24, 25]. In particular, this problem has been extensively investigated in the Fibonacci superlattices which are regarded as a typical example of aperiodic systems [26, 27, 28]. In these studies, it has been found that the wave functions of one-particle states are critical, i.e. nor extended neither localized [29]. Further studies have shown that the decay of the envelope wave function obeys the power law and its structure can be regarded as a multifractal resembling the case of electronic

---

[*] woloszyn@agh.edu.pl

wave functions in disordered systems at the mobility edge [1, 2, 30]. The shape of the wave function is highly fragmented in the finite Fibonacci superlattice, and in the limit of infinite Fibonacci superlattice corresponds to a self-similar Cantor set with zero Lebesgue measure [31, 32].

The purpose of this work is to examine the effect of the nonlinear dynamics of the energy levels driven by weak electric field on the global as well as local electronic structure of the finite semiconductor Fibonacci superlattice made of two different semiconductor layers. Energy spectrum of this superlattice is particularly interesting in weak electric fields where anticrossings lead to closing of the energy gaps [33, 34, 35]. Particular attention is paid to the effect of this nonlinear dynamics of energy levels on spatial fluctuations of the electronic wave function amplitudes and their spatial extents.

In the systems with broken translational symmetry the multifractal analysis provides deep insight into the nature of the electronic wave function [36, 37, 38, 39, 40, 41, 42, 43] and allows to explore the localization phenomena in the presence of the electric field.

Although the results of the present work are related to the semiconductor superlattice, they can be also generalized to other aperiodic superlattices, e.g. photonic or phononic band gap structures under influence of appropriate perturbations [44, 45].

The paper is organized as follows. In Sec. 2, we present the model of the Fibonacci superlattice and the methods of its analysis, in Sec. 3, we present the results and discussion, and the conclusions are presented in Sec. 4.

2 Model of the Fibonacci superlattice and the methods of analysis

We consider the semiconductor aperiodic superlattice generated according to the Fibonacci sequence of two different semiconductor layers made of $Al_{0.3}Ga_{0.7}As$ and GaAs [13, 22]. The differences in the bandgaps of $Al_{0.3}Ga_{0.7}As$ and GaAs semiconductor layers lead to the discontinuities in the conduction as well as valence band edge profiles at the interfaces [46]. This creates the effective potential energy that consists of the set of barriers and potential wells distributed along the growth axis of the semiconductor superlattice (Fig. 1).

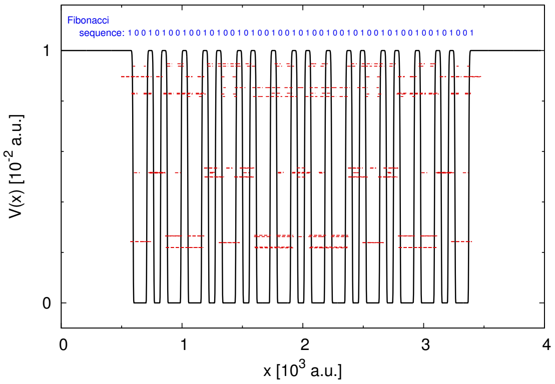

Figure 1: (Colour online) Potential energy profile of the Fibonacci superlattice formed by 20 layers of $Al_{0.3}Ga_{0.7}As$ and 31 layers of GaAs for without the external electric field. The subsequent layers are composed following the Fibonacci binary sequence, i.e. each $Al_{0.3}Ga_{0.7}As$ or GaAs layer corresponds to 1 or 0 in the sequence, respectively. The electronic states are plotted as (red) horizontal lines at their energies, with lines plotted for those x at which $|\psi_n^2(x)|$ exceeds its average value.

The conduction-band potential energy $V(x)$ is modelled by the superposition of the power-exponential potentials in the form [47]

$$V(x) = \sum_{i=1}^{N} V_0 \exp\left[- \left| \frac{x - x_i}{c} \right|^p \right], \qquad (1)$$

where N is the number of $Al_{0.3}Ga_{0.7}As$ barriers located at positions x_i and having height V_0, with parameters c and p characterizing the shape of barriers. The positions of barriers, x_i, are distributed according to the binary Fibonacci sequence generated over set $\{0, 1\}$ using the following inflation rules [48, 49]: $0 \longrightarrow 01$, and $1 \longrightarrow 0$. These rules allow us to obtain the sequence $(0, 1, 0, 0, 1, 0, 1, 0, 0, 1, 0, \ldots)$ of any desired length. In our notation 1 corresponds to $Al_{0.3}Ga_{0.7}As$ layer (barrier) and 0 corresponds to a single GaAs layer having the same width as the barrier.

The envelope wave function of one-particle electronic eigenstate of the Fibonacci superlattice can be found by the solution of the Schrödinger equa-

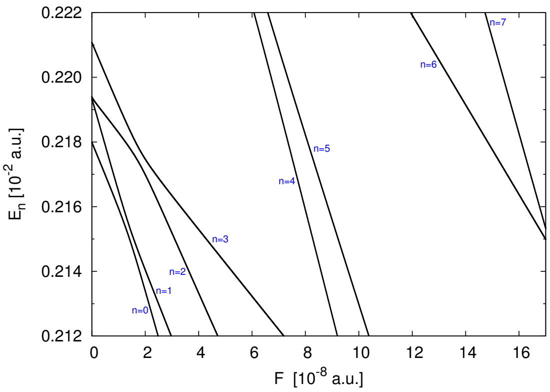

Figure 2: (Colour online) The motion of the eight lowest eigenvalues ($n = 0, 1, .., 7$) driven by the electric field in the finite Fibonacci superlattice formed by 20 layers of $\mathrm{Al}_{0.3}\mathrm{Ga}_{0.7}\mathrm{As}$ and 31 layers of GaAs.

tion within the effective mass approximation

$$-\frac{\hbar^2}{2m^*}\frac{\mathrm{d}^2}{\mathrm{d}x^2}\psi(x) + V(x)\psi(x) = E\psi(x), \qquad (2)$$

where m^* is the effective mass of the conduction band electron.

The Schrödinger equation (2) with the potential energy $V(x)$ given by equation (1) and the Dirichlet boundary conditions, $\psi(0) = \psi(L) = 0$ (where L is the size of the computational box), constitutes the eigenvalue problem which can be solved numerically. This form of the boundary conditions allows us to neglect the complexity of the energy spectrum due to the surface states.

The energy spectrum of the Fibonacci superlattice formed from a finite number of barriers and quantum wells is characterized by the density of states which can be expressed as follows

$$\mathrm{DOS}(E) = \sum_n \delta(E - E_n). \qquad (3)$$

This quantity gives only global properties of the system, whereas the local properties can be described by the local density of states which directly explores the local amplitude of the electronic wave function for a given energy. The local density of states (LDOS) is defined by the formula

$$\mathrm{LDOS}(x, E) = \sum_n |\psi_n(x)|^2 \delta(E - E_n), \qquad (4)$$

where $\psi_n(x)$ is the normalized electronic wave function of the n-th eigenstate.

One of the most characteristic properties of the electronic states in the finite Fibonacci superlattice are the self-similar spatial fluctuations of the electronic wave function amplitude which stem from the aperiodic distribution of the barriers and wells in the system. These fluctuations can be analyzed by the multifractal formalism which allows one a deeper insight into their nature. An essential ingredient of the multifractal formalism is the normalized probability measure of the wave function in the k-th box B_k of linear size ε,

$$P_{nk}(\varepsilon) = \int_{B_k(\varepsilon)} \mathrm{d}x\, |\psi_n(x)|^2. \qquad (5)$$

The multifractal analysis of the electronic wave functions in the Fibonacci superlattice can be performed efficiently by applying the box-counting procedure [50, 51] with condition: $a \ll \varepsilon \ll L$ (a is the lattice constant). The normalized q-th moment of the probability measure of the wave function is given by the formula

$$\mu_{nk}(\varepsilon; q) = \frac{P^q_{nk}(\varepsilon)}{\sum_{j=1}^{N(\varepsilon)} P^q_{nj}(\varepsilon)}, \qquad (6)$$

where $N(\varepsilon) = L/\varepsilon$ is the number of boxes.

For each value of the scaling index q we can determine the singularity strength according to the formula

$$\alpha_n(q) = \lim_{\delta \to 0} \frac{\sum_{k=1}^{N(\varepsilon)} \mu_{nk}(\varepsilon; q) \ln \mu_{nk}(\varepsilon; 1)}{\ln \delta} \qquad (7)$$

and the corresponding singularity spectrum in a parametric representation as follows

$$f(\alpha_n) = \lim_{\delta \to 0} \frac{\sum_{k=1}^{N(\varepsilon)} \mu_{nk}(\varepsilon; q) \ln \mu_{nk}(\varepsilon; q)}{\ln \delta}, \qquad (8)$$

where $\delta = \varepsilon/L$ is the ratio of the box size to the system size.

The singularity spectrum $f(\alpha_n)$ gives an accurate description of the multifractal properties of the probability measure of the wave function. Instead of the singularity spectrum, we can equivalently consider a hierarchy of generalized dimensions of the wave function. It stems from the fact that the generalized dimension $D_n(q)$ is related to the singularity spectrum by the formula

$$D_n(q) = \frac{f(\alpha_n) - q\alpha_n(q)}{1-q}. \tag{9}$$

For the integer values of the scaling index q, the generalized dimensions of the wave function have a physical meaning [52]. A particularly interesting generalized dimension corresponds to $q = 2$ when it is known as the correlation dimension of the wave function. Its significance results from the relation to the density-density correlation function and the inverse participation ratio (IPR) which is a measure of the spatial extent of the eigenstate and can be used to describe the localization properties of the electronic eigenstates in real space [53]. It is an important point since the localization length cannot be defined through the exponential spatial decay of the electronic wave function in the finite aperiodic or disordered superlattices. This fact is a consequence of the strong spatial fluctuations of electronic wave function amplitude and therefore a more adequate description is based on the spatial extension of the wave functions given by the IPR parameter [49, 54, 55],

$$\mathrm{IPR}_n = \int_0^L dx\, |\psi_n(x)|^4. \tag{10}$$

A combination of equations (7), (8) and (9) leads to the relation between the generalized dimension of the electronic wave function and the scaling exponent, $\tau_n(q)$, for the q-th moment of the probability measure [43], namely

$$\tau_n(q) = D_n(q)(1-q). \tag{11}$$

Deviation of the scaling exponent from the linear function of q signals the multifractality of the electronic state.

In the limit of weak electric field, the interband transitions can be neglected and the influence of the electric field on the electronic states of Fibonacci superlattice can be considered by including an additional perturbation in the form

$$W = -eFx\,, \tag{12}$$

where e is the elementary charge, and F is the external homogeneous electric field applied along the growth axis of the system.

In fact, the weak electric field is treated nonperturbatively as a parameter which produces the motion of the energy levels as it is shown in Figure 2. For the considered superlattice the level repulsion leads to the formation of anticrossings in the energy spectrum, which is a simple consequence of the dimensionality of the system and the Dirichlet boundary conditions applied to the Schrödinger equation.

Introducing the perturbation to the Schrödinger equation (2) finally leads to the equation

$$-\frac{\hbar^2}{2m^*}\frac{\mathrm{d}^2}{\mathrm{d}x^2}\psi(x) + [V(x) - eFx]\psi(x) = E\psi(x), \tag{13}$$

which allows us to investigate the effect of weak electric field on the global (energy spectrum, DOS) as well as local properties (LDOS, spatial fluctuations of the wave function amplitude) of the finite Fibonacci superlattice.

3 Numerical results and discussion

Using the model of the finite Fibonacci superlattice described in Sec. 2 we have investigated its global as well as local electronic properties in the limit of weak electric field. All numerical values of the physical quantities which are considered here are given in the atomic units, i.e., $\hbar = |e| = m_0 = 1$. The parameters of the model potential defined in equation (1) are taken to be $V_0 = 0.27$ eV $= 0.01$ a.u., $c = 1.5$ nm $= 28.3$ a.u., and $p = 10$, which means that the system consists of $\mathrm{Al_{0.3}Ga_{0.7}As}$ barriers having width of 3 nm and separated by GaAs layers of 3 nm or 6 nm width (the latter in case of two consecutive zeros in the Fibonacci binary sequence). The number of barriers is $N = 100$ and the constant effective mass approximation is used with the value of m^* equal $0.067m_0$.

One of the characteristic features of the obtained energy spectrum is the presence of minibands with fractal structure (Fig. 3). When the electric field is increased these minibands become broader, with a nonuniform distribution of the energy levels occurring during the entire process. It is the reason why darker and lighter areas corresponding to dense and rare subsets of the levels are present within the bands in Figure 3 showing the influence of the elec-

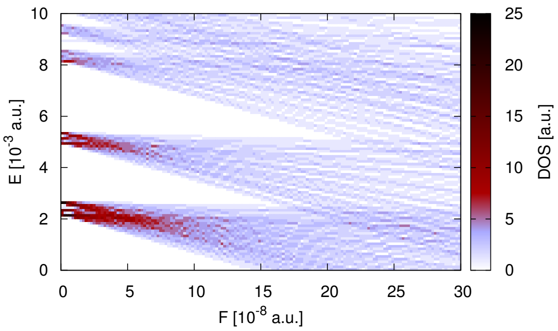

Figure 3: (Colour online) Density of states (DOS) as a function of energy E and electric field F. The results for the Fibonacci superlattice with $N = 100$.

tric field on the DOS of the Fibonacci superlattice. On the other hand, the general structure of the LDOS is not altered and the effect of the electric field is restricted to the change of the slope along the horizontal axis (see Figure 4 presenting how the electric field modifies LDOS, which leads to the previously mentioned broadening of the minibands).

The presence of the anticrossings between the energy levels is the direct cause of the nonuniform structure of the energy spectrum as well as the density of states function [35]. In the region of anticrossings, the electronic wave functions change the degree of localization measured by the IPR parameter. Figure 5 shows the IPR parameter for electronic eigenstates of the Fibonacci superlattice as a function of electric field. The lowest degree of localization is observed in the absence of the electric field, but in contrast to finite periodic systems the localization degree is not simply increasing with the electric field. In case of the finite Fibonacci superlattice the observed behaviour is much more complex. Instead of the successive states with very similar IPR dependence on the electric field, we can notice that for a chosen value of the electric field the highly localized states are separated by the states with much weaker localization.

Therefore, the electric field affects the degree of localization, which in turn results in the change of the spatial fluctuations of the wave function. In order to explain the relation between the increasing electric field and the modification of the spa-

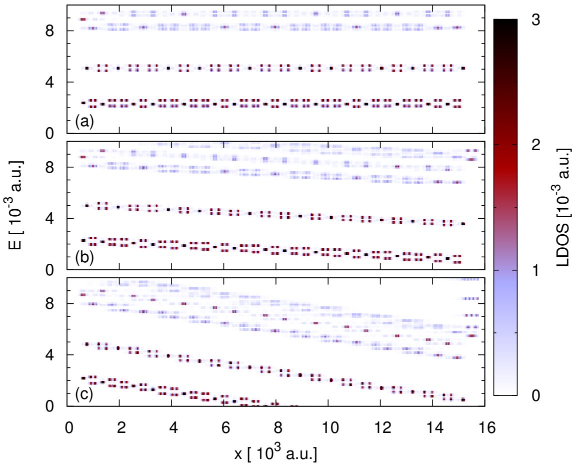

Figure 4: (Colour online) Local density of states LDOS for the Fibonacci superlattice with $N = 100$ as a function of energy E and position x. (a) $F = 0$, (b) $F = 10^{-7}$ [a.u.] and (c) $F = 3 \times 10^{-7}$ [a.u.].

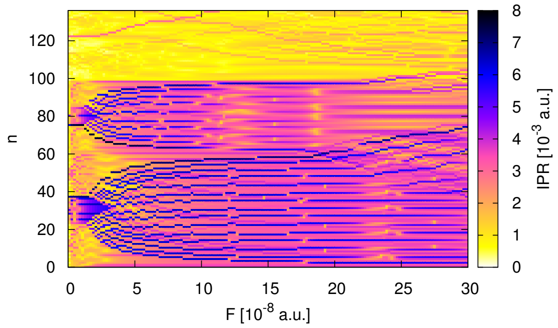

Figure 5: (Colour online) Inverse participation ratio IPR calculated for $n = 0, \ldots, 136$ (i.e. for all eigenstates ψ_n which are bound for $F = 0$) in case of the Fibonacci superlattice with $N = 100$.

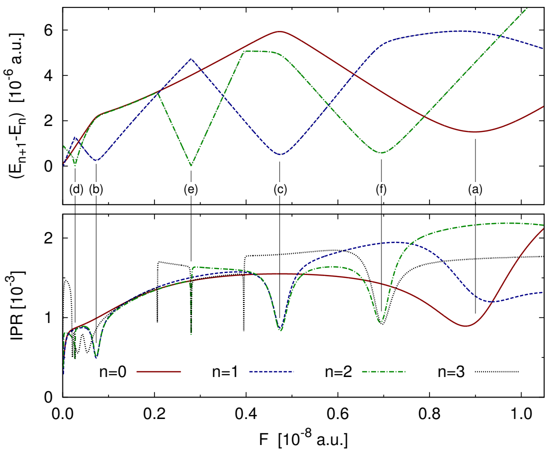

Figure 6: (Colour online) Differences $(E_{n+1} - E_n)$ between the energies of the four lowest subsequent levels (upper panel) and the corresponding values of the inverse participation ratio IPR (lower panel) in the case of $N = 100$ Fibonacci superlattice. Letters (a)-(f) denote the positions of anticrossings.

tial fluctuations of the wave functions we have performed a detailed analysis of the lowest energy levels, i.e. the ground-state level and the first two excited state levels. It should be noted, that each level is changed not only by the external electric field, but also by the coupling to the nearest energy levels. As a result, a nonlinear dependence of the energy levels on the electric field is observed.

The distances between the energy levels n and $n + 1$, calculated for $n = 0, 1, 2$, are presented in Figure 6. The neighbouring states tend to change their positions in such a way that the distances between them increase or decrease alternately. This kind of analysis may be also generalized for higher energy levels, however, in this case a large number of anticrossings is observed which makes the analysis not particularly suitable for the purpose of the clear explanation of the phenomenon. For this reason the further discussion focuses on the regions of anticrossings labelled by (a)-(f) in Figure 6.

Figure 6 presents also the values of IPR parameter calculated for the corresponding states in the same range of the electric field. For the values of the electric field at which the anticrossings are observed, i.e. values of $(E_{n+1} - E_n)$ have minima, also the values of IPR parameter for n and $n + 1$ have local minima. It means that the electronic wave functions matching those levels become less localized and occupy a larger region of space due the coupling between the closely lying levels.

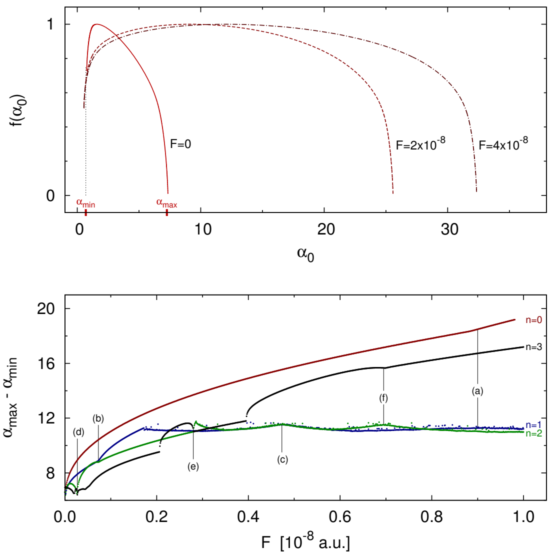

Figure 7: (Colour online) Upper panel: Multifractal spectrum $f(\alpha_n)$ calculated for the ground level state $n = 0$ at different values of the electric field F with $\alpha_{\min}$ and $\alpha_{\max}$ indicated for $F = 0$. Lower panel: The difference between the maximal and minimal singularity strengths, $\alpha_{\max} - \alpha_{\min}$, for the first four lowest energy levels, $n = 0, 1, 2, 3$, with letters (a)-(f) denoting the positions of anticrossings (see also Figure 6).

The further study of the properties of electronic wave functions corresponding to the chosen states is based on the multifractal analysis. The values of the singularity strength α_n and the corresponding singularity spectrum $f(\alpha_n)$, parametrized by the electric field, defined in equations (7) and (8), are calculated using the standard 'box-counting' procedure repeated for the values of the electric field changing from 0 up to 10^{-8}a.u.

The $f(\alpha_n)$ spectrum for the Fibonacci superlattice is found to be strongly asymmetric when no electric field is applied, as it is shown for $n = 0$ in Figure 7. However, while $f(\alpha_n)$ is broadened when the electric field is present, the minimal value of the singularity strength, $\alpha_{\min}$, remains almost constant and close to zero, which is its minimal possible value. This fact may be connected with the nature of the discussed eigenfuctions, which have the localized peaks almost not affected by the increasing electric field, as it can be seen in Fig. 4. Similar behaviour is observed also for higher eigenstates (see the lower panel of the Figure 7), and resembles freezing of the $\alpha_{\min}$ value occurring in disordered systems [56].

As a result, the value $(\alpha_{\max} - \alpha_{\min})$ is not an objective measure of the electronic wave function localization [57] in the case of this type of Fibonacci sequence-based systems under influence of the electric field, which is clearly visible from the comparison with the values of the IPR parameter calculated for the same states (Fig. 6). Moreover, the first derivative of $(\alpha_{\max} - \alpha_{\min})$ is not continuous at the values of the electric field where the anticrossings between the energy levels are observed. In light of these results, we rather think that for this kind of systems, the value $(\alpha_{\max} - \alpha_{\min})$ can be used to detect the local minima of the IPR parameter or equivalently to detect the anticrossings in the energy spectrum.

The multifractal character of the electronic wave function in the finite Fibonacci superlattice and the influence of the weak electric field becomes much more visible in Figure 8, where the q dependence of the scaling exponent, $\tau_n(q)$, for a few lowest electronic states is presented. In all cases the scaling exponent is a convex function, monotonically increasing with q. The electric field modifies the slopes of the considered scaling exponents: to a larger extent for negative q, whereas for positive values of q the changes of the slope are much smaller. This type of changes of the slopes is related to marginal values of the singularity strength [2], $\alpha_{\min}$ (being almost constant as a function of the electric field) and $\alpha_{\max}$ (increasing notably in the electric field).

Changes of $D_n(q)$ in the electric field are also noteworthy, as it is shown in Figure 9. In general, $D_n(q)$ decreases nonlinearly with q and reaches a constant for $q \to -\infty$, however the value strongly depends on the state number on the other hand. For $q \to +\infty$, $D_n(q)$ tends to a constant value, but the dependence of this value on the electronic state is rather weak. The nonlinear decrease of $D_n(q)$ with increasing q is a presage of the wave function multifractality [43].

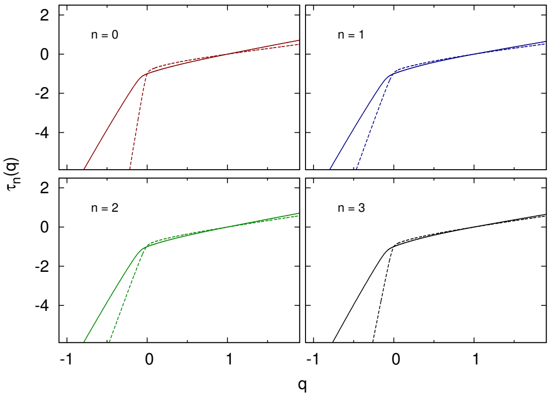

Figure 8: (Colour online) The scaling exponent $\tau_n(q)$ for the electric field $F = 0$ (solid line) and $F = 2 \times 10^{-8}$ (dashed line) and for states $n = 0, 1, 2, 3$.

In the following discussion we present results obtained for $1 < q < 3$ which is the range where the fluctuations are mostly pronounced. Figure 9 shows the generalized dimension calculated in the vicinity of the anticrossings marked in Figure 6. $D_n(q)$ decreases with q, but it has maxima when analyzed as a function of the electric field. The maximal values of $D_n(q)$ appear at the same values of the electric field as the anticrossings and are accompanied by the minima of IPR parameter. It leads to the conclusion that the maximum of the generalized dimension $D_n(q)$ as a function of the electric field corresponds to the decrease of the wave function localization degree. Moreover, if we analyze the surfaces of $D_n(q)$ for both states involved in the anticrossing and plot them as functions of q and the electric field F, it turns out that they cross and this crossing does not take place at the same value of the electric field for all values of q. The curve defined by the crossings that joins points for which the generalized dimensions are the same for the two discussed states, corresponds to the equality of the generalized moments μ_{nk} of the probability densities of the electronic states which are equivalent to the intensity fluctuations [58].

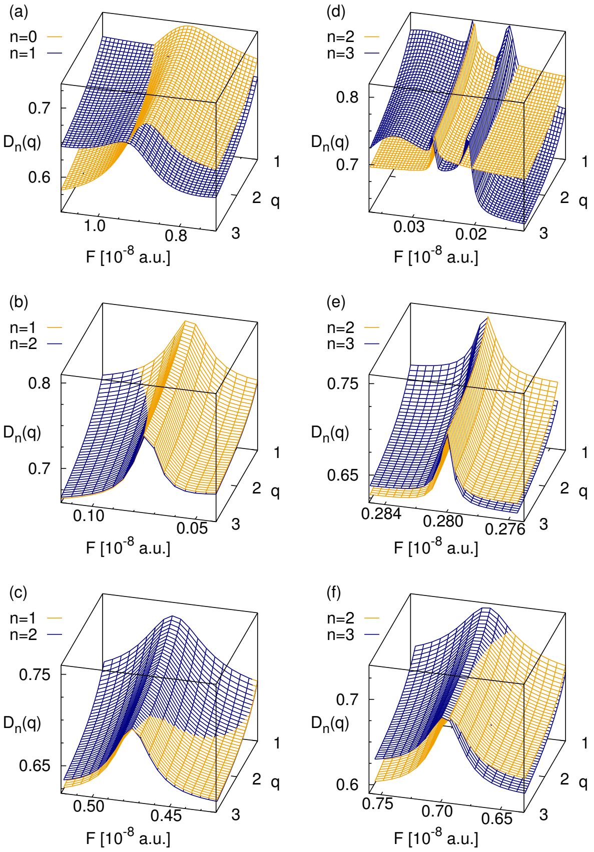

Figure 9: (Colour online) Generalized dimension $D_n(q)$ calculated in the vicinities of the anticrossings (a-f) shown in Figure 6.

4 Concluding Remarks

In the present paper, we have investigated the influence of the weak homogeneous electric field on the one-electron states in the finite superlattice generated according to the Fibonacci sequence of two types of semiconductor layers. For clarity of presented analysis only a few lowest-energy eigenstates have been considered in details, but conclusions can be generalized for higher-energy eigenstates.

We have shown that the nonlinear character of the energy levels dynamics results from the large number of anticrossings. Therefore the energy spectrum of the Fibonacci superlattice and the density of states are nonuniform in the limit of weak electric field. In the vicinity of the anticrossings, the inverse participation ratio of the electronic wave functions for individual electronic eigenstates possesses minima. These minima of the inverse participation ratio are related to the maxima of generalized dimension calculated as a function of electric field, that are observed for $0 < q < 3$ in the vicinity of the anticrossings. Moreover, we have shown that the change of the spatial extent of the electron wave function in the vicinity of the anticrossings is preceded by the correlation between the spatial fluctuations of wave functions corresponding to the electronic eigenstates participating in the anticrossings.

The relation between the positions of anticrossings and the properties of the singularity spectrum has been revealed, and the difference between the maximal and minimal values of the singularity strength has been found not to be a proper measure of the spatial extents of electronic wave functions in the presented case. Quite surprisingly, we have found the discontinuity of the first derivative of the difference between marginal values of the singularity strength for the values of the electric field where the local minima of inverse participation ratio exist. We have also shown that a strong asymmetry of the singularity spectrum is preserved for all considered values of the electric field, although the electric field modifies the shape of the spectrum. This analysis of the relations between the singularity spectrum and the scaling exponents, together with the calculated generalized dimensions, have allowed us to show that the multifractal character of the electronic wave functions in this type of Fibonacci sequence-based systems is not destroyed by the weak electric field.

The results presented above correspond mainly to one arbitrarily chosen length of the Fibonacci sequence used as a basis for the model potential. Our further numerical studies performed for several different sizes of the systems show that the same characteristic features are observed, and thus we have decided to choose a typical example allowing the detailed analysis.

We hope that the presented results can be useful in a deeper understanding of the nonlinear properties of the energy spectrum in the aperiodic photonic, phononic or semiconductor superlattices under influence of an appropriate external perturbation and motivate the experimental verification of the results.

Acknowledgement

Supported by the Polish Ministry of Science and Higher Education and its grants for Scientific Research.

References

[1] A.D. Mirlin, Phys. Rep. **326**, 259 (2000)

[2] F. Evers, A.D. Mirlin, Rev. Mod. Phys. **80**, 1355 (2008)

[3] T. Guhr, A. Müller-Groeling, H.A. Weidenmüller, Phys. Rep. **299**, 189 (1998)

[4] M. Jansssen, Phys. Rep. **295**, 1 (1998)

[5] Z.I. Alferov, Rev. Mod. Phys. **73**, 767 (2001)

[6] H. Kroemer, Rev. Mod. Phys. **73**, 783 (2001)

[7] M. Milun, P. Pervan, D.P. Woodruff, Rep. Prog. Phys. **65**, 99 (2002)

[8] A. Fert, Rev. Mod. Phys. **80**, 1517 (2008)

[9] E. Macia, Rep. Prog. Phys. **69**, 397 (2006)

[10] Y.K. Vekilov, M.A. Chernikov, Phys.-Usp **53**, 537 (2010)

[11] J.M. Luck, H. Orland, U. Smilansky, J. Stat. Phys. **53**, 551 (1988)

[12] A. Endo, Y. Iye, Phys. Rev. B **78**, 085311 (2008)

[13] R. Merlin, K. Bajema, R. Clarke, F.Y. Juang, P.K. Bhattacharya, Phys. Rev. Lett. **55**, 1768 (1985)

[14] K. Järrendahl, M. Dulea, J. Birch, J.E. Sundgren, Phys. Rev. B **51**, 7621 (1995)

[15] A. Chomette, B. Deveaud, A. Regreny, G. Bastard, Phys. Rev. Lett. **57**, 1464 (1986)

[16] F. Laruelle, B. Etienne, Phys. Rev. B **37**, 4816 (1988)

[17] D. Toet, M. Potemski, Y.Y. Wang, J.C. Maan, L. Tapfer, K. Ploog, Phys. Rev. Lett. **66**, 2128 (1991)

[18] D. Munzar, L. Bocaek, J. Humlicek, K. Ploog, J. Phys. Condens. Matter **6**, 4107 (1994)

[19] A. Yamaguchi, T. Saiki, T. Tada, T. Ninomiya, K. Misawa, T. Kobayashi, M. Kuwata-Gonokami, T. Yao, Solid State Commun. **75**, 955 (1990)

[20] N.D. Lanzillotti-Kimura, A. Fainstein, B. Jusserand, A. Lemaître, O. Mauguin, L. Largeau, Phys. Rev. B **76**, 174301 (2007)

[21] V. Passias, N.V. Valappil, Z. Shi, L. Deych, A.A. Lisyansky, V.M. Menon, Opt. Express **17**, 6636 (2009)

[22] T. Taguchi, Y. Yamada, MRS Proceedings **161**, 199 (1989)

[23] M.G. Karkut, J.M. Triscone, D. Ariosa, O. Fischer, Phys. Rev. B **34**, 4390 (1986)

[24] H.Q. Yuan, U. Grimm, P. Repetowicz, M. Schreiber, Phys. Rev. B **62**, 15569 (2000)

[25] T. Rieth, M. Schreiber, J. Phys. Condens. Matter **10**, 783 (1998)

[26] J. Arriaga, V.R. Velasco, J. Phys. Condens. Matter **9**, 8031 (1997)

[27] V.R. Velasco, phys. stat. sol. (b) **232**, 71 (2002)

[28] Z. Aziz, S. Bentata, R. Djelti, Y. Sefir, Solid State Commun. **150**, 865 (2010)

[29] L. Kroon, E. Lennholm, R. Riklund, Phys. Rev. B **66**, 094204 (2002)

[30] C. Castellani, L. Peliti, J. Phys. A **19**, L429 (1986)

[31] M. Kohmoto, L.P. Kadanoff, C. Tang, Phys. Rev. Lett. **50**, 1870 (1983)

[32] M. Kohmoto, B. Sutherland, C. Tang, Phys. Rev. B **35**, 1020 (1987)

[33] P. Carpena, Phys. Lett. A **231**, 439 (1997)

[34] F. Salazar, G. Naumis, J. Phys. Condens. Matter **22**, 115501 (2010)

[35] B.J. Spisak, M. Wołoszyn, Phys. Rev. B **80**, 035127 (2009)

[36] J. Martin, I. García-Mata, O. Giraud, B. Georgeot, Phys. Rev. E **82**, 046206 (2010)

[37] A.D. Mirlin, Y.V. Fyodorov, A. Mildenberger, F. Evers, Phys. Rev. Lett. **97**, 046803 (2006)

[38] E. Cuevas, Phys. Rev. B **68**, 024206 (2003)

[39] E. Cuevas, V.E. Kravtsov, Phys. Rev. B **76**, 235119 (2007)

[40] S. Faez, A. Strybulevych, J.H. Page, A. Lagendijk, B.A. van Tiggelen, Phys. Rev. Lett. **103**, 155703 (2009)

[41] V.E. Kravtsov, A. Ossipov, O.M. Yevtushenko, E. Cuevas, Phys. Rev. B **82**, 161102 (2010)

[42] Y.V. Fyodorov, A. Ossipov, A. Rodriguez, J. Stat. Mech. **2009**, L12001 (2009)

[43] W. Pook, M. Jansssen, Z. Phys. B **82**, 295 (1991)

[44] Y. El Hassouani, H. Aynaou, E.H. El Boudouti, B. Djafari-Rouhani, A. Akjouj, V.R. Velasco, Phys. Rev. B **74**, 035314 (2006)

[45] W. Steurer, D. Sutter-Widmer, J. Phys. D: Applied Physics **40**, R229 (2007)

[46] S.M. Sze, K.N. Kwok, *Physics of Semiconductor Devices* (John Wiley and Sons, Inc., 2007)

[47] M. Ciurla, J. Adamowski, B. Szafran, S. Bednarek, Physica E **15**, 261 (2002)

[48] A. Bovier, J.M. Ghez, Commun. Math. Phys. **158**, 45 (1993)

[49] B.J. Spisak, M. Wołoszyn, Acta Phys. Pol. B. **38**, 1951 (2007)

[50] A. Chhabra, R.V. Jensen, Phys. Rev. Lett. **62**, 1327 (1989)

[51] K.J. Falconer, *Fractal geometry: mathematical foundations and applications* (Wiley, 2003)

[52] H.G.E. Hentschel, I. Procaccia, Physica D **8**, 435 (1983)

[53] B. Huckestein, Rev. Mod. Phys. **67**, 357 (1995)

[54] F. Wegner, Z. Phys. B **36**, 209 (1980)

[55] D.J. Thouless, Phys. Rep. **13**, 93 (1974)

[56] Y.V. Fyodorov, Physica A **389**, 4229 (2010)

[57] P. Biswas, P.K. Thakur, Phys. Lett. A **262**, 464 (1999)

[58] V.N. Prigodin, B.L. Altshuler, Phys. Rev. Lett. **80**, 1944 (1998)